Assessment of Coastal Zone Changes and Relative Bathymetry in Dingalan, Aurora Using Remote Sensing Techniques

Christian Jan I. Alonzo[1] , Gabriel Angelo M. Rondin[1], Jeark A. Principe[1] , Ayin M. Tamondong[1]

[1]Department of Geodetic Engineering, University of the Philippines Diliman, Quezon City, Philippines – (cialonzo, gmrondin, japrincipe, amtamondong)@up.edu.ph

Keywords: Land Cover Change, Shoreline Change, Relative Bathymetry, QSCAT, SCP, Dingalan

Abstract

This study examines the coastal dynamics of Dingalan, Aurora, Philippines, using geospatial tools such as remote sensing and GIS for evaluating land cover changes, shoreline movement, and relative bathymetry. Analysis of Sentinel-2 imagery reveals significant transitions in land cover classes over the years, indicative of the impacts of natural processes and human activities on the coastal landscape. Notably, built-up areas expanded by 175,975.34 m² (33.12%) from 2016 to 2020 and by another 32,365.52 m² (4.58%) from 2020 to 2024. During the same periods, vegetation cover experienced a decrease of 13.01% and 10.22%, respectively. These trends underscore the importance of balanced land use planning to mitigate the environmental impacts of rapid urbanization in coastal zones. Shoreline change detection using Landsat imagery reveals that the eastern portion has been stable throughout the years. In contrast, central and western portions show sediment accumulation, with mean Endpoint Rate and Linear Regression Rate values of 0.97 and 0.98 in the central portion, and 0.79 and 0.82 in the western portion. This highlights the diverse dynamics of shoreline evolution in the area. The relative nearshore bathymetry was calculated using the natural logarithm ratio of blue-to-green spectral bands, yielding values from -0.28 to 0.22, which provide insights into the underwater topography and supports the characterization of shallow-water regions. This study contributes to a deeper understanding of coastal dynamics, providing information essential for effective coastal management and resilience planning in Dingalan and similar regions. It highlights the need for proactive measures to address ongoing environmental changes and underscores the significance of informed coastal management strategies in promoting sustainable development.

1. Introduction

The coastal zone of Dingalan, Aurora, Philippines, presents a dynamic environment influenced by natural processes and human activities. Understanding the changes occurring in this coastal area is essential for effective coastal management and resilience planning. Dingalan, situated on the eastern coast of Luzon Island, boasts diverse coastal ecosystems, including mangroves, beaches, and rocky shores. However, like many coastal regions worldwide, Dingalan faces challenges such as erosion, land use changes, and shoreline alterations due to anthropogenic interventions (Sta. Rita, 2018).

The objective of this research is to analyze changes in land cover and shoreline over time within the coastal area of Dingalan, Aurora, using geospatial tools such as remote sensing and GIS (Abualtayef et al., 2021). It further seeks to explore the relative bathymetry of the study area to enhance the understanding of coastal dynamics and support informed decision-making for coastal management in the Philippine context.

Recent studies have highlighted notable transformations in the coastal regions throughout the Philippines. Coastal change detection along the urban coastline of Metro Manila revealed a decrease of approximately 1.5 kilometers over a 30-year period, attributed to rapid population increase and urbanization (Limbo-Dizon et al., 2023). Similarly, variations in land cover and land use along the coastline of La Union were examined, revealing an evolving coastal landscape in the region (Rivera et al., 2024).

In this study, satellite imagery and GIS tools are employed to conduct three main analyses: land cover change detection, shoreline change detection, and relative bathymetric extraction. Through these analyses, the researchers aim to identify temporal trends and spatial patterns in land cover, shoreline evolution, and bathymetric variations, providing valuable insights for coastal zone management.

2. Methodology

The methodology adopted in this research combines geospatial approaches involving remote sensing and GIS to examine changes in land cover, shoreline position, and relative bathymetry within the coastal area of Dingalan, Aurora (Fig. 1). This integrated framework enables a detailed analysis by utilizing satellite images from multiple time periods together with geospatial processing techniques.

Figure 1. Spatial extent of the study area.

The research utilizes Sentinel-2 and Landsat satellite data to examine the spatiotemporal dynamics of the coastal environment. Fig. 2 illustrates the general workflow applied in this study. Figs. 3 to 8 display the true-color composites of the Sentinel-2 and Landsat datasets analyzed in the research.

Sentinel-2 data were obtained from the Copernicus Open Access Hub, while Landsat data were downloaded from the USGS Earth Explorer platform. A review of related literature was conducted to identify effective methodologies for achieving the study's objectives. The analysis for this study was performed using QGIS plugins, and ArcGIS Pro 3.4 was utilized for map preparation and layout.

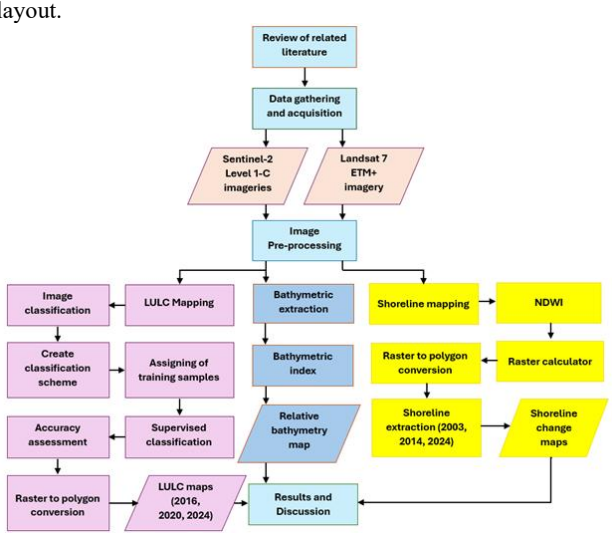

Figure 2. Overview of the methodological framework used in the study.

Figure 3. Sentinel-2 true-color composite of the study area from October 25, 2016.

Figure 4. Sentinel-2 true-color composite of the study area from November 23, 2020.

Figure 5. Sentinel-2 true-color composite of the study area from March 7, 2024.

Figure 6. True-color Landsat 7 ETM+ image of the study area obtained on February 17, 2003.

Figure 7. True-color Landsat 8 OLI image of the study area obtained on February 7, 2014.

Figure 8. True-color Landsat 8 OLI image of the study area obtained on March 6, 2024.

2.1 Land Cover Change Detection

The analysis of land cover changes employed Sentinel-2 Level-1C images from 2016, 2020, and 2024. This dataset was selected mainly for its fine spatial resolution (10 m), which enables detailed identification of land cover categories. Initially, the imagery underwent pre-processing that included atmospheric correction through the Sen2Cor processor (Louis et al., 2016), converting Level-1C products to Level-2A and providing bottom-of-atmosphere reflectance. The Level-2A images were then processed using the Semi-Automatic Classification Plugin (SCP) in QGIS (Congedo, 2023), where they were clipped to match the extent of the study area. During classification, the blue, green, red, and near-infrared spectral bands were selected due to their effectiveness in distinguishing different land cover types.

Training samples representing five classes: sea, vegetation, sediments, bare soil, and built-up were selected for each image corresponding to its respective year. The maximum likelihood algorithm, a supervised classification algorithm, was applied to classify the land cover classes. Following classification, an accuracy assessment was conducted on the classified images in QGIS using the Semi-Automatic Classification Plugin (SCP), with reference data derived from digitized training samples based on historical Google Earth imagery. The resulting classified rasters were then converted to vector format to facilitate the calculation of area per land cover class using the Intersect tool. Land cover changes between the years were subsequently computed.

2.2 Shoreline Change Detection

Since Sentinel-2 has only been operational since 2015, it offers a limited temporal range that restricts long-term shoreline change analysis. To extend the observation period, Landsat data were utilized instead. Specifically, imagery from Landsat 7 Enhanced Thematic Mapper Plus (ETM+) acquired in 2003, and Landsat 8 Operational Land Imager (OLI) acquired in 2014 and 2024, were used for shoreline change assessment. The Normalized Difference Water Index (McFeeters, 1996) was derived from respective spectral bands to produce binary images for each year, which were subsequently converted into vector polygon layers. From these polygons, shorelines were extracted, and a baseline was established by buffering the most recent shoreline by 80 meters. Transects were spaced at 40-meter intervals using the QGIS Shoreline Change Analysis Tool (QSCAT). The tool then computed several shoreline change indicators, namely the Shoreline Change Envelope (SCE), Net Shoreline Movement (NSM), End Point Rate (EPR), and Linear Regression Rate (LRR), to quantify the magnitude and rate of shoreline shifts over time.

$$NDWI = \frac{Green - NIR}{Green + NIR} \quad (1)$$

where
NDWI = Normalized Difference Water Index,
Green = digital number of the green band,
NIR = digital number of the near-infrared band.

2.3 Relative Nearshore Bathymetric Extraction

For the relative bathymetric extraction, a straightforward approach was employed using the natural logarithm ratio of blue-to-green bands from atmospherically corrected Sentinel-2 imagery of the study area in 2024, acquired from the Copernicus Open Access Hub (Copernicus, 2024). This log-ratio approach, based on Stumpf et al. (2003), was applied to derive relative nearshore bathymetric information and assess underwater terrain variations. Despite its simplicity, this analysis provides valuable knowledge of the underwater landscape, complementing the broader understanding of coastal dynamics.

This log-ratio of blue-to-green bands operates on the principle that blue light penetrates water more deeply than green light. In shallower waters, there is more reflectance from the blue band compared to the green band, leading to higher index values. Conversely, in deeper waters, blue-band reflectance decreases more rapidly than green-band reflectance, resulting in lower index values. These index values effectively represent relative bathymetry, distinguishing between shallower and deeper regions without providing exact depth measurements. This method is effective for estimating relative bathymetry in shallow waters and is commonly used in coastal studies due to its simplicity and the widespread availability of multispectral satellite data. It offers a practical approach for environmental monitoring and coastal management, particularly in nearshore environments.

3. Results and Discussion

The results of the study are presented and discussed in the following subsections, encompassing land cover change detection, shoreline change detection, and relative nearshore bathymetric extraction, all of which contribute to a comprehensive understanding of the coastal processes within the study area.

3.1 Land Cover Change Detection

Table 1 summarizes the accuracy assessment results for the land cover classification for the years 2016, 2020, and 2024. These results provide important evaluations of the reliability of the classification. For 2016, the overall accuracy was 98.52%, indicating a high degree of reliability. The producer's accuracy for built-up areas was 96.39%, with a user's accuracy of 98.77%, reflecting the model's strong performance in identifying and classifying built-up areas correctly. However, some built-up and sediment features appeared in the middle of the sea (Fig. 9), which is unlikely to occur. These anomalies may be attributed to the ocean surfaces that display wave foam, which exhibits spectral values similar to built-up and sediment features. This spectral ambiguity can mislead the classifier, resulting in ocean areas being incorrectly classified as built-up or sediment. Recognizing these discrepancies is crucial for refining future analyses and improving the accuracy of land cover change detection. For 2020, the overall accuracy dropped to 86.51%, with the producer's accuracy for built-up areas decreasing to 76.19% and the user's accuracy to 95.81%. This decline suggests some challenges in accurately capturing built-up areas during this period. Lastly, for 2024, the overall accuracy improved to 98.35%, with the producer's accuracy for built-up areas reaching 100% and the user's accuracy at 84.52%. The consistently high accuracy values support the reliability of the change detection results, making the findings dependable for coastal management decision-making.

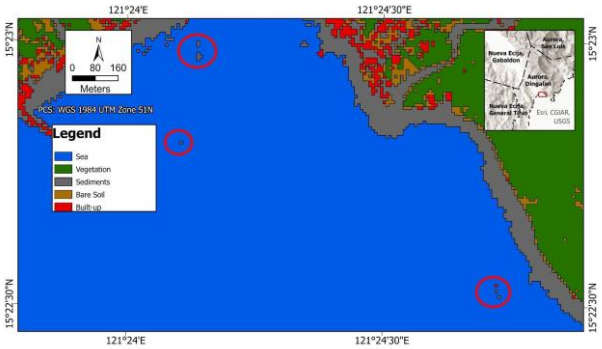

Figure 9. Built-up and sediment features appearing in the 2016 classified map.

Year	Land class	Producer's accuracy (%)	User's accuracy (%)	Overall accuracy (%)
2016	Sea	100.00	100.00	98.52
	Vegetation	99.27	100.00	
	Sediments	100.00	60.00	
	Bare soil	85.71	100.00	
	Built-up	96.39	98.77	
2020	Sea	100.00	100.00	86.51
	Vegetation	98.46	100.00	
	Sediments	96.43	34.18	
	Bare soil	74.00	86.05	
	Built-up	76.19	95.81	
2024	Sea	99.72	100.00	98.35
	Vegetation	96.83	100.00	

	Sediments	99.90	78.99	
	Bare soil	92.49	99.31	
	Built-up	100.00	84.52	

Table 1. Accuracy assessment summary of land cover classification.

The land cover classification results for Dingalan, Aurora, show significant changes in land cover from 2016 to 2024 (Figs. 10-12). The land cover distribution in terms of area and percentage and results of the change detection analysis are summarized in Tables 2 to 4. These results reveal dynamic transitions among various land cover classes, indicating the effects of both natural processes and human activities. The classification was conducted using a substantial number of training samples for each year: 499 samples in 2016, 566 samples in 2020, and 183 samples in 2024 as shown in Table 5. Validation samples were randomly digitized to evaluate the quality of the classification. The number of samples used for the accuracy assessment is displayed in Table 6.

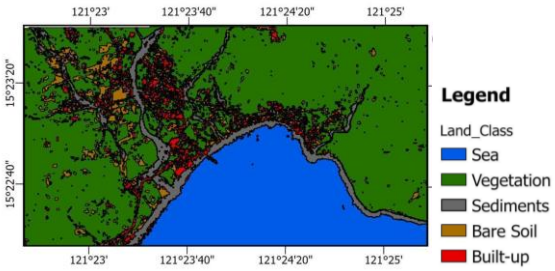

Figure 10. Land cover classification results for 2016.

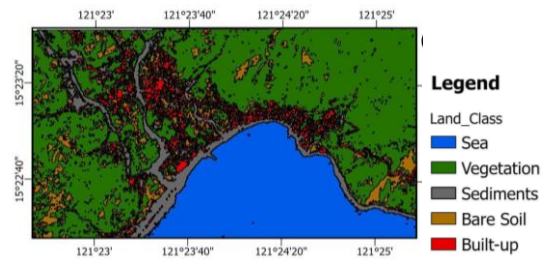

Figure 11. Land cover classification results for 2020.

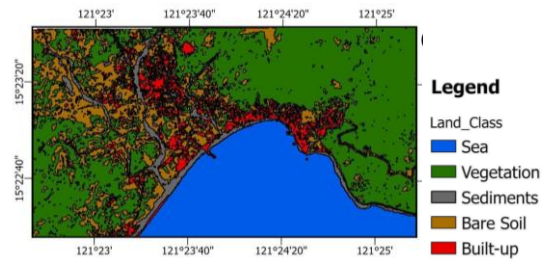

Figure 12. Land cover classification results for 2024.

Class	Area 2016 (m^2)	Area 2020 (m^2)	Area 2024 (m^2)
Built-up	531,310.62	707,285.96	739,651.48
Vegetation	7,407,908.62	6,444,182.42	5,785,358.22
Bare Soil	1,081,247.74	1,635,901.19	2,594,469.69
Sediments	1,085,621.41	1,362,821.03	887,501.65
Sea	2,877,913.60	2,833,810.94	2,977,020.80
Total:	12,984,001.99	12,984,001.54	12,984,001.84

Table 2. Land cover area (m^2) for the years 2016, 2020, and 2024.

Class	Area 2016 (%)	Area 2020 (%)	Area 2024 (%)
Built-up	4.09%	5.45%	5.70%
Vegetation	57.05%	49.63%	44.56%
Bare Soil	8.33%	12.60%	19.98%
Sediments	8.36%	10.50%	6.84%
Sea	22.17%	21.83%	22.93%
Total:	100.00%	100.00%	100.00%

Table 3. Percentage distribution of land cover for the years 2016, 2020, and 2024.

Land cover change (2016 - 2020)	Area change (m^2)	Percent change (%)
Bare Soil - Built-up	164,593.86	15.22
Bare Soil - Sediments	252,002.18	23.31
Bare Soil - Vegetation	347,041.58	32.1
Built-up - Bare Soil	73,104.71	13.76
Built-up - Sea	600.04	0.11
Built-up - Sediments	156,410.05	29.44
Built-up - Vegetation	57,398.50	10.8
Sea - Bare Soil	NA	NA
Sea - Built-up	100.01	0
Sea - Sediments	68,404.50	2.38
Sediments - Bare Soil	90,287.20	8.32
Sediments - Built-up	164,002.52	15.11
Sediments - Sea	23,801.81	2.19

Sediments - Vegetation	84,802.50	7.81
Vegetation - Bare Soil	1,154,899.15	15.59
Vegetation - Built-up	134,792.27	1.82
Vegetation - Sediments	163,276.92	2.2

Land cover change (2020 - 2024)	**Area change (m^2)**	**Percent change (%)**
Bare Soil - Built-up	109,604.46	6.7
Bare Soil - Sediments	110,201.13	6.74
Bare Soil - Vegetation	759,692.31	46.44
Built-up - Bare Soil	231,992.22	32.8
Built-up - Sea	1,600.10	0.23
Built-up - Sediments	122,195.66	17.28
Built-up - Vegetation	19,697.54	2.78
Sea - Bare Soil	100.01	0
Sea - Built-up	1,000.08	0.04
Sea - Sediments	1,800.14	0.06
Sediments - Bare Soil	367,896.27	27
Sediments - Built-up	222,691.98	16.34
Sediments - Sea	144,509.98	10.6
Sediments - Vegetation	40,702.59	2.99
Vegetation - Bare Soil	1,338,077.91	20.76
Vegetation - Built-up	74,554.52	1.16
Vegetation - Sediments	66,284.50	1.03

Land cover change (2016 - 2024)	**Area change (m^2)**	**Percent change (%)**
Bare Soil - Built-up	144,868.39	13.4
Bare Soil - Sediments	159,104.76	14.71
Bare Soil - Vegetation	202,003.27	18.68
Built-up - Bare Soil	151,806.81	28.57
Built-up - Sea	8,300.53	1.56
Built-up - Sediments	109,002.60	20.52
Built-up - Vegetation	19,298.90	3.63
Sea - Bare Soil	100.01	0
Sea - Built-up	900.07	0.03
Sea - Sediments	1,300.10	0.05
Sediments - Bare Soil	245,101.05	22.58
Sediments - Built-up	200,407.93	18.46
Sediments - Sea	93,106.84	8.58
Sediments - Vegetation	36,092.91	3.32
Vegetation - Bare Soil	1,622,190.50	21.9
Vegetation - Built-up	150,573.30	2.03
Vegetation - Sediments	107,181.53	1.45

Table 4. Land cover changes from 2016 to 2020, from 2020 to 2024, and from 2016 to 2024.

Class	**Year**		
	2016	**2020**	**2024**
Ocean	80	113	48
Vegetation	218	236	25
Sediments	100	59	36
Bare soil	24	74	32
Built-up	77	84	42
Total	499	566	183

Table 5. Land cover classification training samples.

Class	**Year**		
	2016	**2020**	**2024**
Ocean	20	20	21
Vegetation	20	20	21
Sediments	20	20	35
Bare soil	20	20	16
Built-up	20	20	21
Total	100	100	114

Table 6. Land cover classification validation samples.

This contribution has been peer-reviewed. The double-blind peer-review was conducted on the basis of the full paper.
https://doi.org/10.5194/isprs-annals-X-5-W4-2025-27-2026 | © Author(s) 2026. CC BY 4.0 License.

Between 2016 and 2020, the most notable change was the transformation of vegetation to bare soil, with an area of 1,154,899.15 m^2 (15.59%) undergoing this change. This indicates a negative trend in vegetation cover, potentially due to land clearing, urban expansion, or other forms of environmental disturbance. The built-up land area also expanded significantly, with 164,593.86 m^2 (15.22%) of bare soil converting to built-up areas. This trend continued from 2020 to 2024, as built-up areas expanded further, transforming 109,604.46 m^2 (6.70%) of bare soil and 74,554.52 m^2 (1.16%) of vegetation into built-up land.

For built-up areas, the data show a consistent increase over the eight-year period. From 2016 to 2020, built- up areas expanded by 175,975.34 m^2 (33.12%), and from 2020 to 2024, they increased by another 32,365.52 m^2 (4.58%). This significant growth in built-up areas highlights ongoing urbanization and infrastructure development in the coastal zone of Dingalan. Such expansion may lead to various environmental impacts, including increased runoff and potential loss of biodiversity. The change detection analysis also reveals a notable increase in bare soil, particularly from 2020 to 2024, when 1,338,077.91 m^2 (20.76%) of bare soil replaced vegetation. Additionally, vegetation cover in the area significantly decreased by 13.01% from 2016 to 2020, indicating possible deforestation. This trend continued from 2020 to 2024, though at a slightly lower rate (10.22%), suggesting a need for mitigation strategies to prevent further forest loss.

3.2 Shoreline Change Detection

A comprehensive shoreline change analysis within the study area was conducted using Landsat 7 ETM+ imagery for 2003 and Landsat 8 imagery for 2014 and 2024. NDWI was applied to generate binary images, which were then converted into vector polygons for shoreline extraction and baseline construction. Fig. 13 shows the extracted shorelines for 2003, 2014, and 2024 along with the constructed baseline. Transects were delineated at 40-meter intervals (Fig. 14).

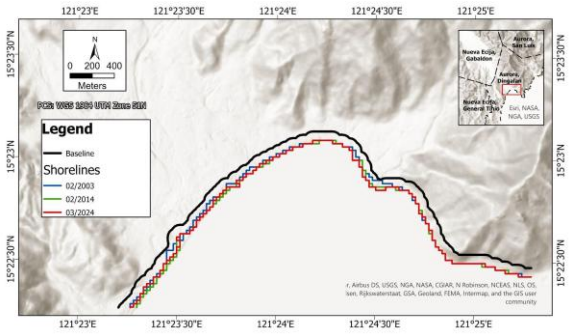

Figure 13. Digitized shoreline for the years 2003, 2014, 2024, and the constructed baseline.

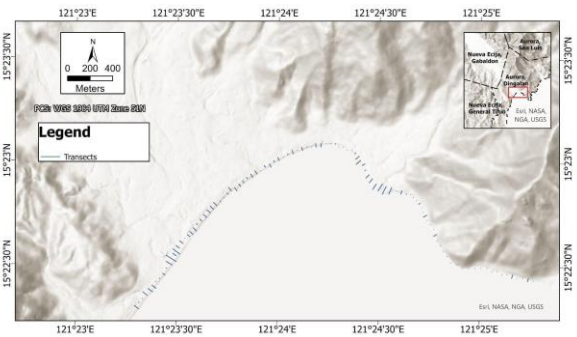

Figure 14. Cast transects along the shoreline.

Statistical analysis further illustrates the complexity of shoreline change, with metrics such as Shoreline Change Envelope (SCE), Net Shoreline Movement (NSM), Endpoint Rate (EPR), and Linear Regression Rate (LRR) used to quantify the magnitude and direction of change (Figs. 15-18). SCE quantifies the range of variability in shoreline position over a specified time period. NSM calculates the difference between the shoreline's endpoints, indicating the overall direction and magnitude of movement. Moreover, EPR measures the average annual rate of change at specific endpoints along the shoreline. Lastly, LRR employs a linear regression model to estimate the rate of shoreline change over time, facilitating the identification of long-term trends. The eastern portion of the shoreline, with mean EPR and LRR values of 0.04, shows modest results across all metrics, indicating minimal net movement or stability over the study period, in line with the visual assessment of shoreline positions. The central and western sections exhibit dominant values indicating significant shoreline change. In the central portion, mean EPR and LRR values of 0.97 and 0.98, respectively, indicate increasing accretion or progradation. Similarly, the western section is characterized by mean values of 0.79 for EPR and 0.82 for LRR, suggesting consistent trends of shoreline advancement.

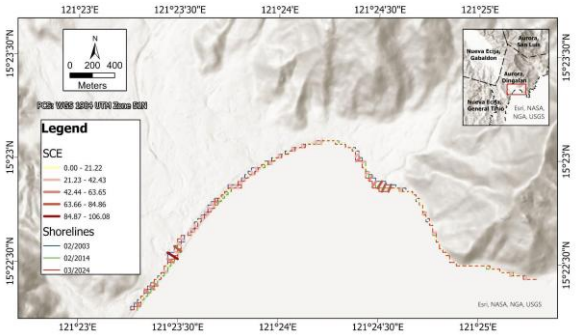

Figure 15. Shoreline change envelope (SCE) statistical analysis.

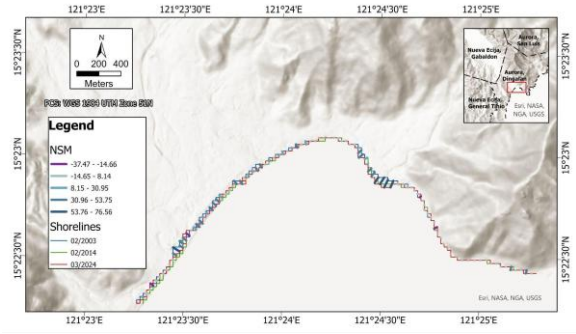

Figure 16. Net shoreline movement (NSM) statistical analysis.

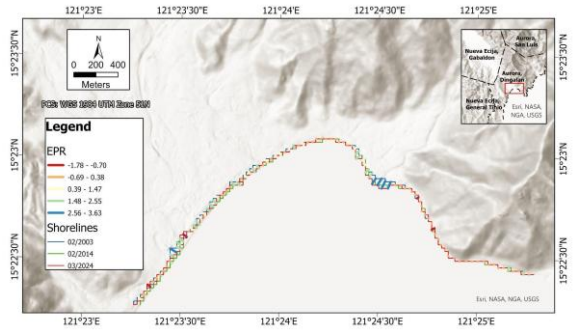

Figure 17. End Point Rate (EPR) statistical analysis.

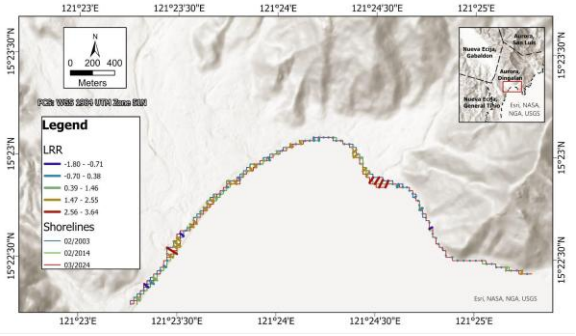

Figure 18. Linear Regression Rate (LRR) statistical analysis.

3.3 Relative Nearshore Bathymetric Extraction

The output raster of the bathymetric index shows pixel values ranging from -0.28 to 0.22, indicating depth variations within the study area (Fig. 19). Deeper parts of the ocean exhibit lower index values, while shallower regions display higher index values. The gradient effectively maps the relative depth of the nearshore waters, providing valuable insights into the underwater topography of the area.

Shoreline progradation in the central and western sections corresponds to areas where the bathymetric index values show a sharp transition from shallow to deep, indicating a steep underwater slope. This sharp gradient can reduce wave energy near the shore and promote sediment deposition, helping the shoreline to advance. In contrast, the eastern section shows more uniform index values, reflecting a gentler seabed slope. This stable underwater profile likely allows wave energy to dissipate more evenly, resulting in minimal shoreline change.

The combined analysis of land cover change, shoreline dynamics, and nearshore bathymetry in Dingalan, Aurora, reveals a linked system where terrestrial and marine processes influence each other. Rapid urban expansion and vegetation loss affect sediment supply and runoff, contributing to the observed shoreline progradation in the central and western zones, where steeper nearshore slopes promote sediment deposition. In contrast, the gentler eastern slopes correspond with shoreline stability. These relationships underscore the need for integrated coastal management that considers land use planning, shoreline protection, and bathymetric conditions to maintain coastal stability and resilience.

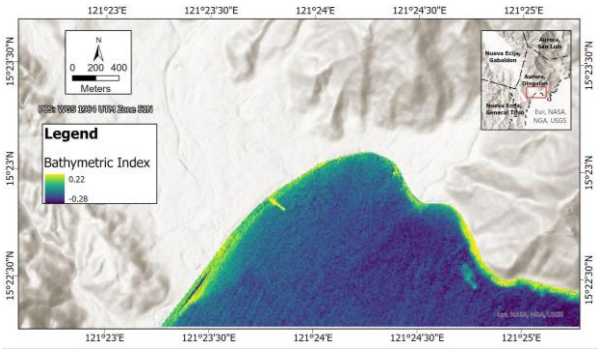

Figure 19. Relative nearshore bathymetry map of the area.

4. Conclusion and Recommendations

Based on a comprehensive remote sensing and GIS-based analysis of the coastal zone of Dingalan, Aurora, Philippines, this research provides valuable findings into the land cover dynamics, shoreline changes, and relative bathymetry of the area. The land cover change detection analysis revealed significant transitions among various land cover classes over the years, reflecting the impacts of both natural processes and anthropogenic activities on the coastal landscape. Notably, built-up areas expanded by 175,975.34 m² (33.12%) from 2016 to 2020 and by another 32,365.52 m² (4.58%) from 2020 to 2024. During the same periods, vegetation cover experienced a decrease of 13.01% and 10.22%, respectively. These trends underscore the importance of balanced land use planning to mitigate the environmental impacts of rapid urbanization in coastal zones. Additionally, shoreline change detection using Landsat imagery reveals that the central and western portions of the shoreline in the study area are experiencing sediment accumulation, with mean EPR and LRR values of 0.97 and 0.98 in the central portion, and 0.79 and 0.82 in the western portion. The relative nearshore bathymetric extraction using the log-ratio of blue-to-green bands provided valuable insights into the underwater topography, enabling the characterization of shallow and deep-water regions within the study area. The resulting index values ranged from -0.28 to 0.22, revealing a gentle nearshore slope in the eastern portion and steeper nearshore zones in the central and western portions. This pattern is consistent with the observed relative shoreline stability in the eastern area and shoreline advancement in the central and western areas.

For future studies, it is recommended to incorporate tidal data when selecting the date and time for image acquisition to ensure a more reliable shoreline change analysis. Moreover, if available, use fine- or high-resolution imagery to improve the accuracy and precision of the land cover classification and shoreline delineation. Finally, obtaining true depth values is recommended to facilitate regression analysis for relative nearshore bathymetric extraction.

The findings of this study can support local government units (LGUs) and coastal planners in identifying priority areas for shoreline protection, vegetation conservation, and sustainable land use zoning. The observed link between urban expansion, vegetation loss, shoreline dynamics, and bathymetric profiles highlights the need for integrated coastal zone management strategies. Incorporating these results into hazard mapping, climate adaptation plans, and environmental monitoring programs will enable decision-makers to more effectively balance development goals with the preservation of coastal resilience in Dingalan and similar coastal environments.

References

Abualtayef, M., Abd Rabou, M., Afifi, S., Abd Rabou, A.F., Seif, A.K., Masria, A. 2021: Change detection of Gaza coastal zone using GIS and remote sensing techniques. *Journal of Coastal Conservation*, 25(36). https://doi.org/10.1007/s11852-021-00825-4

Congedo, L. 2023: Semi-Automatic Classification Plugin (SCP) for QGIS (Version compatible with QGIS 3.28). Available at: https://fromgistors.blogspot.com/p/semi-automatic-classification-plugin.html

Copernicus, 2024: Sentinel-2 satellite imagery. European Space Agency. Available at: https://scihub.copernicus.eu

Esri, 2024: ArcGIS Pro 3.4. Available at: https://pro.arcgis.com/en/pro-app/latest/get-started/download-arcgis-pro.htm

Limbo-Dizon, J.E., Dagamac, N.H.A. 2023: Assessment of coastal change detection on an urban coastline: A case study in metropolitan Manila, Philippines. *IOP Conference Series: Earth and Environmental Science*, 1165, 012015. https://doi.org/10.1088/1755-1315/1165/1/012015

Louis, J., Debaecker, V., Pflug, B., Main-Knorn, M., Bieniarz, J., Mueller-Wilm, U., Cadau, E., & Gascon, F. (2016). SENTINEL-2 SEN2COR: L2A Processor for users. Living Planet Symposium, 740, 91. https://elib.dlr.de/107381/

McFEETERS, S. K. (1996). The use of the Normalized Difference Water Index (NDWI) in the delineation of open water features. International Journal of Remote Sensing, 17(7), 1425–1432. https://doi.org/10.1080/01431169608948714

QGIS Development Team, 2024: QGIS Geographic Information System (Version 3.28). Available at: https://qgis.org

QScat Plugin Developers, 2024: QScat Plugin for QGIS (Version compatible with QGIS 3.28), February 2024. Available at: https://plugins.qgis.org/plugins/qscat/ [accessed 05 May 2024]

Rivera, P.C., Amik, J.E., Escobar, M.I., Olfato-Parojinog, A., Sobremonte-Maglipon, P.A., Limbo-Dizon, J.E., Dagamac, N.H. 2024: Land Use/Land Cover Change along the Coastline of La Union, Philippines. *Journal of Geomatics*, 18(1). https://doi.org/10.58825/jog.2024.18.1.129

Sta. Rita, K.S.C. 2018. Geomorphologic Characterization of Dingalan Town Proper and Barangays in Its Proximity: Implications for Infrastructure Development and Sustainable Land Usage. *International Journal of Scientific & Engineering Research, 9*(9), pp. 708–799. ISSN 2229-5518

Stumpf, R.P., Holderied, K., Sinclair, M. 2003: Determination of water depth with high-resolution satellite imagery over variable bottom types. *Limnology and Oceanography*, 48(1), 547–556. https://doi.org/10.4319/lo.2003.48.1_part_2.0547